

## Interference effects in nonanalog pion double charge exchange

M. G. McKinzie, H. T. Fortune, P. Hui, R. Ivie, C. Laymon, X. Li, S. Loe,  
D. A. Smith, and A. L. Williams

*University of Pennsylvania, Philadelphia, Pennsylvania 19104*

J. M. O'Donnell

*Los Alamos National Laboratory, Los Alamos, New Mexico 87545*

S. Blanchard, G. R. Burleson, and B. Lail

*New Mexico State University, Las Cruces, New Mexico 88003*

(Received 5 August 1993)

For  $(\pi^+, \pi^-)$  double charge exchange on  $^{27}\text{Al}$ , an excitation function at  $5^\circ$  has been measured over a range of incident pion energies from 100 to 293 MeV for transitions to both the ground state and to a doublet at 1.75 MeV of excitation in the final nucleus  $^{27}\text{P}$ . The shapes of these excitation functions are strikingly different, with the g.s. data exhibiting an interferencelike dip near 150 MeV and the excited state falling smoothly above 150 MeV.

PACS number(s): 25.80.Gn

### I. INTRODUCTION

The pion double charge exchange (DCX) reaction leading to discrete final states has been studied extensively over the  $\Delta_{33}$  resonance region. Those data, consisting of  $5^\circ$  excitation functions and, for several nuclei, forward angular distributions, permit categorization of the exhibited DCX trends in excitation function and angular distribution by the character of the transition. All existing DCX data to low-lying final states may be separated into three classes: (1) double isobaric analog transitions (DIAT); (2) nonanalog ground-state-to-ground-state transitions with  $J_i^\pi = J_f^\pi = 0^+$  (NA I), and the remaining nonanalog transitions (NA II) which include data from  $T = \frac{1}{2}$  targets and transitions to excited states from  $T = 0, 1$  targets. The DIAT and NA I transitions have well-defined, contrasting systematics. Less is known of NA II transitions, which are the subject of this paper.

All  $5^\circ$  DIAT excitation functions are consistent with a rise in cross section from  $T_\pi = 180$  to 292 MeV. Below 180 MeV there is a range of behavior [1–8]. By contrast, all NA I excitation functions at  $5^\circ$  exhibit a peak near  $T_\pi = 165$  MeV, averaging about 80 MeV wide [9–12]. Whereas the DIAT exhibits simple features above resonance, but complicated target-related behavior below 180 MeV, NA I transitions exhibit the same features for different targets at all energies.

The third and least studied category of DCX reactions includes both DCX on  $T = \frac{1}{2}$  targets and transitions to excited states from  $T = 0, 1$  targets. Nonanalog ground-state-to-ground-state excitation functions have been measured on the  $T = \frac{1}{2}$  nuclei  $^9\text{Be}$  [11,13] and  $^{13}\text{C}$  [11,14]. For low-lying excited states, DCX has been previously measured for the  $T = 0$  nuclei  $^{12}\text{C}$  [15] and  $^{16}\text{O}$  [12], the  $T = 1$  nuclei  $^{14}\text{C}$  [4,16] and  $^{18}\text{O}$  [1,2], and for the  $T = \frac{1}{2}$  nucleus  $^{13}\text{C}$  [14,16]. For the DIAT, two analog sequential charge exchanges to the final state are allowed

and expected, in first order, to dominate. The NA I reactions necessarily involve two nonanalog routes in the DCX transition. However, for the majority of measurements within the NA II category, if  $T_i \neq 0$ , nonanalog DCX can proceed via two sequential single charge exchanges (SCX) in which one is an isobaric analog transition. Unlike DIAT and NA I,  $\Delta J^\pi$  values different from  $0^+$  are permitted and probably dominant for NA II DCX.

### II. CURRENT EXPERIMENT

The measurements were performed with the Energetic Pion Channel and Spectrometer (EPICS) [17] at the Clinton P. Anderson Meson Physics Facility (LAMPF) with the standard pion DCX setup [1]. A chemically pure aluminum target of  $1.8 \text{ g/cm}^2$  areal density was used to obtain data for this experiment at  $5^\circ$  for nine energies from  $T_\pi = 100$  to 293.4 MeV. Electron rejection was facilitated by using a series of five Cherenkov detectors in the focal plane filled with isobutane gas. For incident pion energies from 140 to 293.4 MeV, muon events were ranged out via a scintillator placed behind a series of aluminum and graphite wedges. In addition, time-of-flight measurements permitted the separation of muon and electron from pion events below 140 MeV. In this manner, background not arising from continuum DCX on the Al target was largely eliminated from the fully analyzed histograms.

The spectrometer acceptance was measured using relative yields of inelastic scattering to the 4.44-MeV state of  $^{12}\text{C}$ . The spectrometer field was varied to move the  $^{12}\text{C}$   $2^+$  state across the focal plane, covering  $\pm 10\%$  of the central momentum of the spectrometer. For selected incident energies, measurements of elastic yields on the Al and  $\text{CH}_2$  targets were performed at two different settings of the central momentum of the spectrometer and under otherwise identical experimental conditions. A system-

atic uncertainty of  $\pm 2.4\%$  was found for the determination of relative yields obtained at different values of particle momenta relative to the spectrometer central momentum. Absolute normalization was obtained by measuring the hydrogen elastic cross section with a  $\text{CH}_2$  target of areal density  $27.7 \text{ mg/cm}^2$  and comparing the yields with cross sections computed from  $\pi$ -nucleon phase shifts [18]. Energy loss in the  $^{27}\text{Al}$  target was measured via elastic scattering at all points of the DCX excitation function to determine reaction  $Q$  values.

Normalized histograms, corrected for target energy losses and the relative spectrometer acceptance, were fitted to obtain a functional expression for the background and peaks of interest. A third-order polynomial was used as an expression for the continuum DCX background. On average, few background counts were observed in the region of the  $^{27}\text{P}$  ground state, forcing the functional expression for the background to terminate at an excitation energy of about 1.5 MeV to obtain a good fit to the data ( $\chi^2_{\text{RED}} \sim 1$ ). Background contributions to the ground-state cross sections were estimated by averaging background events for an equivalent energy interval just below the ground state. Elastic scattering measurements indicated an experimental resolution of 770 keV. The excited state in  $^{27}\text{P}$  was found to be best fitted by a line shape identical in form to the elastic line shape.

### III. RESULTS AND DISCUSSION

Data were taken at a laboratory angle of 5 degrees for nine energies spanning the resonance region from 100 to 293.4 MeV. The spectrum shown in Fig. 1 is the sum of all data over the region of the  $^{27}\text{P}$  ground state and low-lying excited state(s). It has been corrected for energy losses in the target, but not for the acceptance of the spectrometer or the relative normalizations of the data runs at different energies. Cross sections to these states and their measured  $Q$  values are presented in Table I. Those few ground-state events observed at each energy were consistent with the ground-state  $Q$  value calculated from known masses [19]. A spin-parity assignment of  $\frac{1}{2}^+$  for the  $^{27}\text{P}$  ground state is based on comparison with its mirror nucleus  $^{27}\text{Mg}$ . A weighted-average excitation

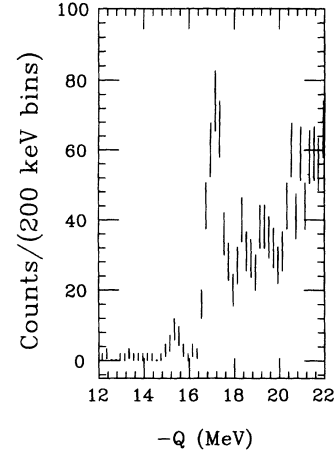


FIG. 1. Missing-mass histogram for  $^{27}\text{Al}(\pi^+, \pi^-)^{27}\text{P}$  for the region in  $Q$  value of the final ground state and excited doublet. Data at all incident energies have been summed.

energy of 1.75 MeV (standard deviation 0.12 MeV) was measured for the excited state in  $^{27}\text{P}$  relative to the calculated ground-state  $Q$  value of  $-15.4237 \pm 0.0035$  MeV. A level diagram for  $^{27}\text{P}$  inferred from  $^{27}\text{Mg}$  identifies the excited state as occurring at the location of a  $\frac{5}{2}^+$  doublet at  $E_x = 1.7, 1.9$  MeV in  $^{27}\text{Mg}$ , separated by over 1 MeV from neighboring excited states. The variation in the measured excitation energy of this state is attributed to its character as an unresolved doublet. Figure 2 contrasts the  $5^\circ$ ,  $^{27}\text{Al}(\pi^+, \pi^-)$  excitation functions to the ground state and excited state, as measured in this experiment.

Of course, the shape of a  $5^\circ$  excitation function may reflect an energy dependence of the angular-distribution shape, so it must be used selectively as a signature for a class of reactions which embraces transitions of potentially different multiplicities. Though at present the data set for NA II transitions is limited, there are some suggestive similarities between excitation functions of a given transition multipolarity.

The dip in the  $^{27}\text{P}(\text{g.s.})$  cross section at  $T_\pi \sim 164$  MeV, for example, is reminiscent of the behavior for the  $^{18}\text{O}(\pi^+, \pi^-)^{18}\text{Ne}(2^+, 1.89 \text{ MeV})$  excitation function [1,2], as displayed in Fig. 2. A smooth curve has been drawn

TABLE I.  $Q$  values and  $5^\circ$  cross sections (c.m.) for  $^{27}\text{Al}(\pi^+, \pi^-)^{27}\text{P}$  measured in this experiment. An asterisk signifies insufficient statistics to establish a centroid at that energy.

$T_\pi$ (MeV)	$^{27}\text{P}(\text{g.s.})$		$^{27}\text{P}(\frac{5}{2}^+ \text{ doublet})$	
	$-Q$ (MeV) <sup>a</sup>	$d\sigma/d\Omega$ (nb/sr)	$-Q$ (MeV) <sup>b</sup> (MeV)	$d\sigma/d\Omega$ (nb/sr)
293.4	$15.37 \pm 0.18$	$12.7 \pm 5.1$	$17.01 \pm 0.14$	$16.2 \pm 5.6$
260.4	$15.59 \pm 0.17$	$7.8 \pm 2.7$	$17.24 \pm 0.15$	$12.3 \pm 3.5$
230	$15.27 \pm 0.22$	$4.1 \pm 2.0$	$17.10 \pm 0.05$	$32.3 \pm 5.1$
200	$15.16 \pm 0.30$	$4.1 \pm 2.4$	$17.02 \pm 0.07$	$30.4 \pm 5.9$
180	*	$3.1 \pm 2.2$	$17.39 \pm 0.06$	$74.0 \pm 10.7$
164	*	$\leq 1.4$	$17.14 \pm 0.03$	$107.8 \pm 12.7$
140	$15.55 \pm 0.21$	$4.3 \pm 1.8$	$17.21 \pm 0.05$	$139.0 \pm 14.8$
120	$15.79 \pm 0.45$	$8.6 \pm 5.5$	$17.24 \pm 0.06$	$137.6 \pm 22.9$
100	*	$\leq 19.4$	*	$\leq 71$

<sup>a</sup> Weighted mean g.s.  $Q$  value =  $-15.445 \pm 0.089$ . Value from the masses is  $-15.424$ .

<sup>b</sup> Weighted mean excited state  $Q$  value =  $-17.17$  with a standard deviation of 0.12 MeV.

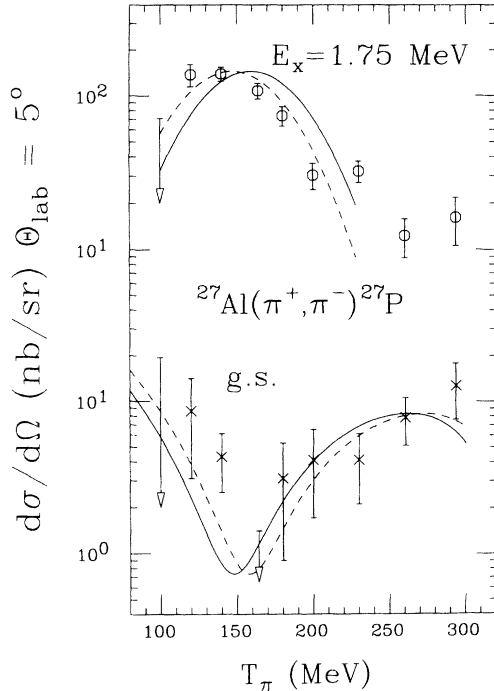


FIG. 2. Excitation functions at  $5^\circ$  to states in the final nucleus  $^{27}\text{P}$  measured in this experiment. A smooth curve has been drawn to match the  $^{18}\text{Ne}(2^+, 1.89 \text{ MeV})$  excitation function, and is compared to the  $^{27}\text{P}(\text{g.s.})$  data without (solid) and with (dashed) an energy shift equal to the difference in  $Q$  value between the two reactions. Likewise a smooth curve has been drawn to match the  $^{16}\text{Ne}(0^+, \text{g.s.})$  data, and is compared to the  $^{27}\text{P}(1.75 \text{ MeV})$  data without (solid) and with (dashed) an energy shift equal to the difference in  $Q$  value between the two reactions.

to match the  $^{18}\text{Ne}$  data, and shifted in energy by the difference in reaction  $Q$  values to give a comparison of cross section at identical out-going pion kinetic energy. The most obvious similarity between the two excitation functions, the minimum near resonance, may be tied to the fact that  $\Delta J^\pi = 0^+$  is permitted for one, but not both, of the sequential single charge exchanges. The  $^{27}\text{P}(\text{g.s.})$  cross section is only about 2.0% of that for  $^{18}\text{Ne}$  (1.89). Some of this reduction undoubtedly arises from distortion factors; SCX isobaric analog state (IAS) cross sections go as  $A^{-4/3}$ , as do those for NA I transitions. Nuclear structure, and  $J$  and  $T$  coupling coefficients, presumably account for additional reduction. Both transitions are probably dominated by a  $d_{3/2}^{5/2} \rightarrow d_{3/2}^{5/2}$  analog transition and a  $d_{3/2}^{5/2} \rightarrow s_{1/2}^{5/2}$  nonanalog step. In  $^{18}\text{Ne}$ , however, the non-analog part of the transition also contains an appreciable  $d_{3/2}^{5/2} \rightarrow d_{3/2}^{5/2}$  component.

The  $^{27}\text{P}(\frac{5}{2}^+, 1.75 \text{ MeV})$  data are compared in Fig. 2 to a smooth curve drawn to match the measured  $5^\circ$  excitation function for the NA I  $^{16}\text{O}(\pi^+, \pi^-)^{16}\text{Ne}$  reaction [1,8,10,22]. A resonance-like shape to the excitation function about  $T_\pi \sim 164 \text{ MeV}$ , as found for NA I excitation functions, does seem to fit the  $^{27}\text{P}(1.75 \text{ MeV})$  excitation function when the centroid of the Lorentzian is shifted by the difference in out-going pion kinetic energy between the  $^{16}\text{O}$  and  $^{27}\text{Al}(\pi^+, \pi^-)$  reactions. We note that the

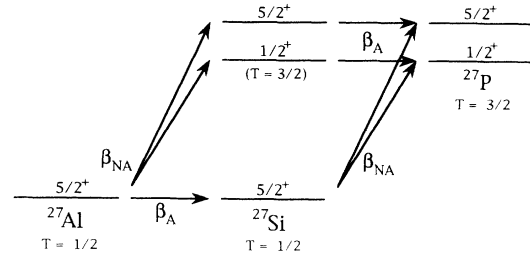


FIG. 3. Postulated reaction paths for two sequential single charge exchanges, in which each path involves one isobaric analog transition. The total DCX amplitude in this schematic diagram is the product of an analog ( $\beta_A$ ) and nonanalog ( $\beta_{NA}$ ) term.

cross section at the maximum of the  $^{27}\text{P}(1.75 \text{ MeV})$  excitation function at  $T_\pi \sim 140 \text{ MeV}$  is only about 50% of that expected from the established mass dependence for NA I cross sections at  $5^\circ$  and 164 MeV [23], perhaps indicative of an interfering amplitude in addition to that which describes a purely nonanalog reaction route.

For  $^{27}\text{Al}(\pi^+, \pi^-)$ , Fig. 3 illustrates the intermediate states of two sequential single charge exchanges for reaction paths in which one transition is an isobaric analog transition. The full expression for this DCX amplitude is probably dominated by the product of an analog and a nonanalog term, where more than one multipolarity can contribute to the latter. Cross sections for  $^{27}\text{Al}(\pi^+, \pi^0)$  SCX to the  $^{27}\text{Si}$  ground state (the isobaric analog state of the  $^{27}\text{Al}$  ground state) have been measured at four incident pion energies from 100 to 500 MeV [20,21]. The cross section rises smoothly from 0.15 mb/sr at  $T_\pi = 100 \text{ MeV}$  to 1.0 mb/sr at 500 MeV. The IAS completely dominates the low-energy portion of the SCX missing-mass histogram. If the DCX on  $^{27}\text{Al}$  proceeds through two sequential single charge exchanges, one step should then be dominated by the IAS transition, which might then determine the shape of the DCX excitation function. However, neither DCX excitation function measured in this experiment is consistent with a fourfold increase in cross section from 100 to 300 MeV, as measured in the SCX.

#### IV. CONCLUSIONS

A  $5^\circ$  excitation function for  $^{27}\text{Al}(\pi^+, \pi^-)^{27}\text{P}$  from  $T_\pi = 100$  to 293.4 MeV has been measured for transitions to both the ground state and an excited state at the position of a doublet in the final nucleus. These cross sections exhibit completely different behaviors. The general shape of the  $5^\circ$  excitation function over the resonance region for NA II transitions may be correlated with macroscopic angular momentum transfer. The contrasting SCX excitation function to the IAS for the same target nucleus indicates the presence of an interfering amplitude in addition to the one describing the SCX reaction to the IAS. This amplitude could depend strongly on the wave functions of the intermediate and final nuclear states.

This work was supported by grants from the National Science Foundation and the Department of Energy.

- [1] S. J. Greene, W. J. Braithwaite, D. B. Holtkamp, W. B. Cottingame, C. F. Moore, G. R. Burleson, G. S. Blanpied, A. J. Viescas, G. H. Daw, C. L. Morris, and H. A. Thiessen, *Phys. Rev. C* **25**, 927 (1982).
- [2] Peter A. Seidl, C. Fred Moore, S. Mordechai, R. Gilman, Kalvir S. Dhuga, H. T. Fortune, J. D. Zumbro, C. L. Morris, J. A. Faucett, and G. R. Burleson, *Phys. Lett.* **154B**, 255 (1985).
- [3] Kamal K. Seth, M. Kaletka, S. Iversen, A. Saha, D. Barlow, D. Smith, and L. C. Liu, *Phys. Rev. Lett.* **52**, 894 (1984).
- [4] Peter A. Seidl, Mark D. Brown, Rex R. Kiziah, C. Fred Moore, Helmut Baer, C. L. Morris, G. R. Burleson, W. B. Cottingame, Steven J. Greene, L. C. Bland, R. Gilman, and H. T. Fortune, *Phys. Rev. C* **30**, 973 (1984).
- [5] R. Gilman, H. T. Fortune, J. D. Zumbro, Peter A. Seidl, C. Fred Moore, C. L. Morris, J. A. Faucett, G. R. Burleson, S. Mordechai, and Kalvir S. Dhuga, *Phys. Rev. C* **33**, 1082 (1986).
- [6] Peter A. Seidl, Rex R. Kiziah, Mark K. Brown, C. Fred Moore, C. L. Morris, Helmut Baer, Steven J. Greene, G. R. Burleson, W. B. Cottingame, L. C. Bland, R. Gilman, and H. T. Fortune, *Phys. Rev. Lett.* **50**, 1106 (1983).
- [7] H. T. Fortune, S. Mordechai, R. Gilman, K. Dhuga, J. D. Zumbro, G. R. Burleson, J. A. Faucett, C. L. Morris, P. A. Seidl, and C. Fred Moore, *Phys. Rev. C* **35**, 1151 (1987).
- [8] P. A. Seidl, M. A. Brown, M. Burlein, G. R. Burleson, Kalvir S. Dhuga, H. T. Fortune, R. Gilman, S. J. Greene, M. A. Machuca, C. Fred Moore, S. Mordechai, C. L. Morris, D. S. Oakley, M. A. Plum, G. Rai, M. J. Smithson, Z. F. Wang, D. L. Watson, and J. D. Zumbro, *Phys. Rev. C* **42**, 1929 (1990).
- [9] L. C. Bland, R. Gilman, M. Carchidi, K. Dhuga, Christopher L. Morris, H. T. Fortune, S. J. Greene, Peter A. Seidl, and C. Fred Moore, *Phys. Lett.* **128B**, 157 (1983).
- [10] R. Gilman, H. T. Fortune, Kalvir S. Dhuga, Peter H. Kutt, L. C. Bland, Rex R. Kiziah, C. Fred Moore, Peter A. Seidl, C. L. Morris, and W. B. Cottingame, *Phys. Rev. C* **29**, 2395 (1984).
- [11] G. R. Burleson, G. S. Blanpied, G. H. Daw, A. J. Viescas, C. L. Morris, H. A. Thiessen, S. J. Greene, W. J. Braithwaite, W. B. Cottingame, D. B. Holtkamp, I. B. Moore, and C. F. Moore, *Phys. Rev. C* **22**, 1180 (1980).
- [12] R. Gilman, Ph.D. thesis, University of Pennsylvania, 1985; Los Alamos National Laboratory Report No. LA-10524-T, 1985.
- [13] K. Seth, in *Intermediate-Energy Nuclear Chemistry Workshop*, Los Alamos, NM, 23–27 June 1980 (Los Alamos National Laboratory Report No. LA-8835-C, 1980), p. 250.
- [14] Peter A. Seidl, Mark D. Brown, Rex R. Kiziah, C. Fred Moore, Helmut Baer, C. L. Morris, G. R. Burleson, W. B. Cottingame, Steven J. Greene, L. C. Bland, R. Gilman, and H. T. Fortune, *Phys. Rev. C* **30**, 1076 (1984).
- [15] S. Mordechai, Peter A. Seidl, C. Fred Moore, L. C. Bland, R. Gilman, Kalvir S. Dhuga, H. T. Fortune, C. L. Morris, and S. J. Greene, *Phys. Rev. C* **32**, 999 (1985).
- [16] P. A. Seidl, Ph.D. thesis, The University of Texas at Austin, 1985; Los Alamos National Laboratory Report No. LA-10338-T, 1985.
- [17] H. A. Thiessen, Los Alamos Scientific Laboratory Report No. LA-6663-MS, 1977 (unpublished).
- [18] G. Rowe, M. Salomon, and Rubin H. Landau, *Phys. Rev. C* **18**, 584 (1978).
- [19] M. S. Antony, J. Britz, and A. Pape, *At. Data Nucl. Data Tables* **40**, 9 (1988).
- [20] Helmut W. Baer, J. D. Bowman, M. D. Cooper, F. H. Cverna, C. M. Hoffman, Mikkel B. Johnson, N. S. P. King, J. Piffaretti, E. R. Siciliano, J. Alster, A. Doron, S. Gilad, M. Moinester, P. R. Bevington, and E. Winkelman, *Phys. Rev. Lett.* **45**, 982 (1980).
- [21] S. H. Rokni, H. W. Baer, A. G. Bergman, J. D. Bowman, F. Irom, M. J. Leitch, C. J. Seftor, J. Alster, E. Piasezky, B. L. Clausen, R. A. Loveman, R. J. Peterson, J. L. Ullmann, J. R. Comfort, J. N. Knudson, and U. Sennhauser, *Phys. Lett. B* **202**, 35 (1988).
- [22] S. J. Greene, W. B. Cottingame, G. R. Burleson, L. C. Bland, R. Gilman, H. T. Fortune, C. L. Morris, D. B. Holtkamp, and C. F. Moore, *Phys. Rev. C* **27**, 2375 (1983).
- [23] R. Gilman, H. T. Fortune, J. D. Zumbro, C. M. Laymon, G. R. Burleson, J. A. Faucett, W. B. Cottingame, C. L. Morris, Peter A. Seidl, C. Fred Moore, L. C. Bland, Rex R. Kiziah, S. Mordechai, and Kalvir S. Dhuga, *Phys. Rev. C* **35**, 1334 (1987).
- [24] R. Gilman, L. C. Bland, Peter A. Seidl, C. Fred Moore, C. L. Morris, Steven J. Greene, and H. T. Fortune, *Nucl. Phys. A* **432**, 610 (1985).